Article

Sparse Inversion for the Iterative Marchenko Scheme of Irregularly Sampled Data

Jingwen Zeng[1], Liguo Han[1,*]

[1] College of Geo-Exploration Science and Technology, Jilin University, Changchun 130026, China;
* Correspondence: hanliguo@jlu.edu.cn

Abstract: The Marchenko method is a data-driven way which makes it possible to calculate Green's functions from virtual points in the subsurface by the reflection data at the surface, only requiring a macro velocity model. This method requires collocated sources and receivers. However, in practice, subsampling of sources or receivers will cause gaps and distortions in the obtained focusing functions and Green's functions. To solve this problem, this paper proposes to integrate sparse inversion into the iterative Marchenko scheme. Specifically, we add sparsity constraints to the Marchenko equations and apply sparse inversion during the iterative process. Our work not only reduces the strict requirements on acquisition geometries, but also avoids the complexity and instability of direct inversion for Marchenko equations. This new method is applied to a two-dimensional numerical example with irregular sampled data. The result shows that it can effectively fill gaps of the obtained focusing functions and Green's functions in the Marchenko method.

Keywords: Marchenko method; irregular sampling; focusing function; Green's function; sparse inversion

1. Introduction

The Marchenko method is a data-driven method. It can bring Green's functions from focal points from the subsurface to the surface, requiring only the reflection response measured at the surface and direct arrivals from focal points to the surface [1-3]. The obtained response doesn't have any internal multiples related to the overburden. Marchenko equations has long been used by mathematical physicists as the basis of one-dimensional inverse scattering theory [4-6]. Broggini and Snieder introduced the Marchenko equation into the field of geophysics [7].

Similarly, Bakulin and Calvert proposed the virtual source method based on seismic interferometry [8]. This method can also retrieve Green's function. However, there should be a physical receiver as the virtual source in the medium. And it requires illumination from both above and below [9]. However, in practice, illumination generally appears only from the top, which means that the retrieved Green's function contains false multiples [10]. In contrast, the Marchenko method does not require a physical receiver inside the medium, and illuminating from one side is sufficient. In a one-dimensional medium, Green's functions between the virtual source in the medium and the receiver at the surface can be retrieved from the reflection response at the surface. Wapenaar et al. extended their work to 2D and 3D media [11]. Wapenaar and da Costa Filho et al. extended the method to elastic media [12-13]. Singh et al. discussed about free surface multiples in this method [14]. Slob made this method applicable to dissipative acoustic media [15]. The Marchenko method has been used for subsurface imaging without internal multiples [16-18] and internal multiple elimination [19-20].

However, there are some challenges related to the Marchenko method. This method requires collocated sources and receivers, low noise, no attenuation effect, and prior knowledge of the source signal. These requirements limit the wide application of the Marchenko method. This paper only discusses the problem of the strict acquisition geometry. For now, various ways are being sought to relax this limitation. Ravasi deduced the Rayleigh Marchenko equation so that the source can be placed at any position relative to the receiver [21]. Peng and Vasconcelos studied the subsampling and aperture limiting effects in the Marchenko method [22]. Wapenaar and IJsseldijk rewrote Marchenko equations considering the case of imperfectly sampling and integrating over the source dimension. They used point spread function and multi-dimensional deconvolution for inversion to restore the distorted focusing functions and Green's functions [23]. Then this new representation of Marchenko equations was integrated into the iterative Marchenko scheme [24]. Haindl et al. considered the case in which subsampling over the source dimension and integrating

Preprints (www.preprints.org) | NOT PEER-REVIEWED | Posted: 5 December 2022 doi:10.20944/preprints202212.0055.v1

over receiver dimension, proposing a sparse inversion method to compensate for the irregularity of the source [25].

In this paper, we fucus on the situation where irregulate sampling and integrating are over different dimensions. We propose to integrate sparse inversion into the iterative Marchenko scheme. Our work compensates for the Marchenko method with irregularly sampled data, reducing the complexity of solving equations directly. This paper is organized as follows: Firstly, we introduce the discrete representations for the Marchenko method, and the problem of this Method caused by irregular sampling. Subsequently, we integrate sparse inversion into the iterative Marchenko scheme and give the workflow of our method. Finally, numerical examples verify the performance of our method. The results show that this method effectively reconstruct obtained focusing functions and Green's functions in the Marchenko method under imperfectly sampling.

2. Methods

2.1. Discrete Representations for the Marchenko Method

We assume a non-uniform lossless acoustic medium. The reflection response of the surface of this medium is given by $R\left(\mathbf{x}_R,\mathbf{x}_S,t\right)$, where $\mathbf{x}_S$ is the position of the source, $\mathbf{x}_R$ is the position of the receiver and t is the time. A focal point $\mathbf{x}_A$ is defined inside the medium. The downgoing and upgoing Green's function from the surface $\mathbb{S}_0$ to this focal point are respectively expressed as $G^{+}\left(\mathbf{x}_A,\mathbf{x}_R,t\right)$ and $G^{-}\left(\mathbf{x}_A,\mathbf{x}_R,t\right)$. The coupled Marchenko equation and Green's functions can be connected by focusing function (Wapenaar et al., 2014):

$$G^{\pm}\left(\mathbf{x}_A,\mathbf{x}_R,t\right)\mp f_1^{\pm}\left(\mathbf{x}_R,\mathbf{x}_A,\mp t\right)=\mp\int_{\mathbb{S}_0}R\left(\mathbf{x}_R,\mathbf{x}_S,t\right)*f_1^{\mp}\left(\mathbf{x}_S,\mathbf{x}_A,\mp t\right)\mathrm{d}\mathbf{x}_S. \quad (1)$$

$f_1^{\pm}\left(\mathbf{x}_R,\mathbf{x}_A,\mp t\right)$ is the defined focusing functions. $\pm$ denotes downgoing ($+$) and upgoing ($-$) propagation. The asterisk indicates a temporal convolution. In practical application, the infinite integral on the right side of Equation 1 is approximated by the finite sum of available sources [23]:

$$\hat{G}^{\pm}\left(\mathbf{x}_A,\mathbf{x}_R,t\right)\mp\hat{f}_1^{\pm}\left(\mathbf{x}_R,\mathbf{x}_A,\mp t\right)=\mp\sum_i R\left(\mathbf{x}_R,\mathbf{x}_S^{(i)},t\right)*f_1^{\mp}\left(\mathbf{x}_S^{(i)},\mathbf{x}_A,\mp t\right)*S\left(t\right), \quad (2)$$

where i is the source position and $S\left(t\right)$ is the source wavelet. Equation 1 is to integrate under the source dimension. Through the source-receiver reciprocity theorem, the equation can be rewritten into the form of integrating under the receiver dimension:

$$G^{\pm}\left(\mathbf{x}_A,\mathbf{x}_S,t\right)\mp f_1^{\pm}\left(\mathbf{x}_S,\mathbf{x}_A,\mp t\right)=\mp\int_{\mathbb{S}_0}R\left(\mathbf{x}_R,\mathbf{x}_S,t\right)*f_1^{\mp}\left(\mathbf{x}_R,\mathbf{x}_A,\mp t\right)\mathrm{d}\mathbf{x}_R. \quad (3)$$

Therefore, Equation 2 is correspondingly modified as follows:

$$\hat{G}^{\pm}\left(\mathbf{x}_A,\mathbf{x}_S,t\right)\mp\hat{f}_1^{\pm}\left(\mathbf{x}_S,\mathbf{x}_A,\mp t\right)=\mp\sum_i R\left(\mathbf{x}_R^{(i)},\mathbf{x}_S,t\right)*f_1^{\mp}\left(\mathbf{x}_R^{(i)},\mathbf{x}_A,\mp t\right)*S\left(t\right). \quad (4)$$

If the source sampling in Equation 2 (or the receiver sampling in Equation 4) is irregular when acquiring reflection data, the sum on the right side will introduce waveform distortions to the focusing functions and Green's functions on the left side. If the receiver sampling in Equation 2 (or the source sampling in Equation 4) is irregular, leaves both waveform distortions and spatial gaps in the obtained focusing functions and Green's functions [22]. More details about both situations are in the next section.

2.2. The Standard Marchenko Method With Irregular Sampling

Let us see the velocity model shown in Figure 1. The reflection response is obtained by 201 co-located sources and receivers with 10 m spacing. The time sampling interval is 4 ms. The seismic wavelet is Ricker wavelet of 20 Hz. The focal point is located at (x = 0 m, z = 950 m). Figures 2a and 2b show the sampling masks for the source and receiver dimensions, respectively, with 40 % of them randomly removed.

The standard Marchenko method is processed according to Equation 4. Figures 3a shows the focusing function with irregularly sampled under the source dimension and integrating under the receiver dimension. Figures 4a is the corresponding Green's function. Figures 3b shows the focusing function with irregularly sampled and integrating both under the receiver dimension. Figures 4b is the corresponding Green's function. As references, Figures 3c is the focusing function under regular sampling, and Figures 4c is the Green's function under regular sampling.

We can see that the focusing function (Figures 3a) and Green's function (Figures 4a) obtained by sampling and integrating under the different dimensions have clear space gaps and artifacts. The

Preprints (www.preprints.org) | NOT PEER-REVIEWED | Posted: 5 December 2022 doi:10.20944/preprints202212.0055.v1

focusing function (Figures 3b) and Green's function (Figures 4b) obtained by sampling and integrating under the same dimension have no gap in space, but artifacts also appear.

This is because when the sampling and integrating are carried out under the same dimension, the obtained focusing functions will become more and more inaccurate in the summation process of each iteration due to the increase of the sampling interval. But it still keeps good sampling in space. When the sampling and integrating are performed on the different dimensions, the focusing functions is accurate in the iterative summation process, but the sampling process will lead to the space gap in the focusing functions. In addition, since the focusing function gaps in the iterative process will carry out into the summation process, the non-zero elements of the focusing functions in the next iteration will be inaccurate [22]. The inaccuracy of the focusing functions lead to the inaccuracy of the subsequent Green's functions.

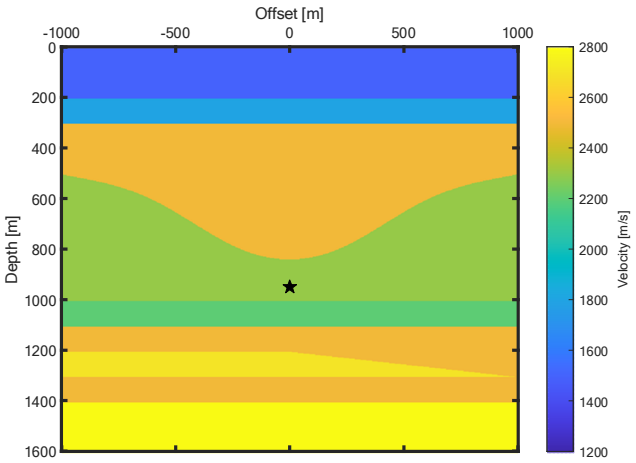

Figure 1. The velocity model. The black star indicates the position of the focal point at (x, z) = (0 m, 950 m).

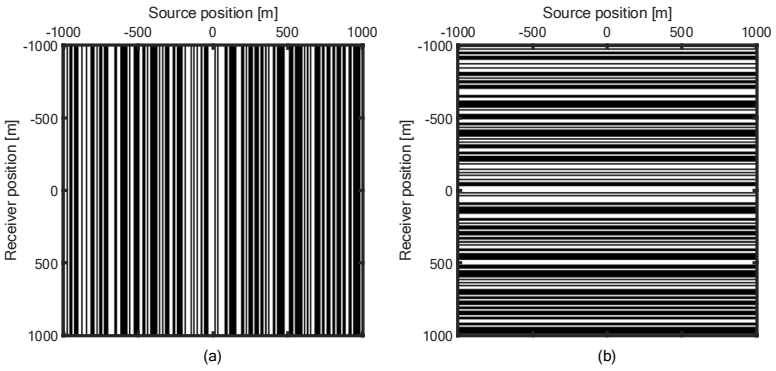

Figure 2. The sampling mask for sampling (a) under the source dimension; (b) under the receiver dimension.

Preprints (www.preprints.org) | NOT PEER-REVIEWED | Posted: 5 December 2022 doi:10.20944/preprints202212.0055.v1

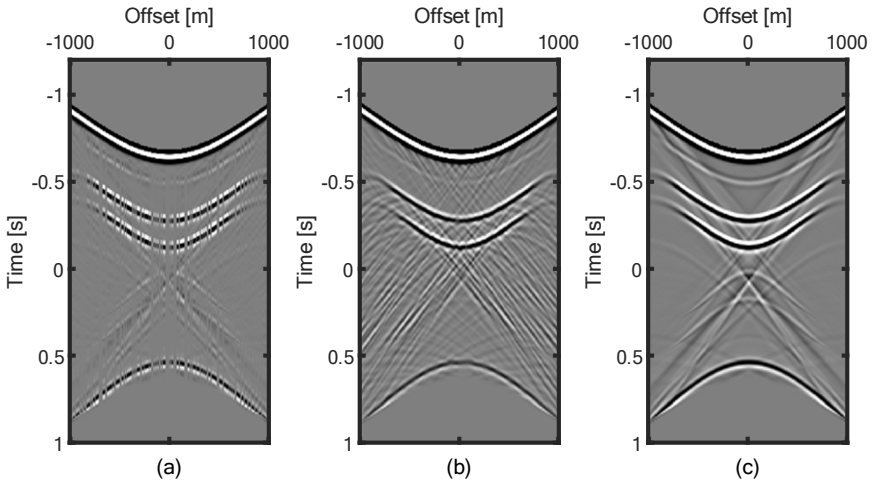

Figure 3. The focusing functions obtained by the standard Marchenko method integrated under the receiver dimension. They are sampled (a) under the source dimension; (b) under the receiver dimension; (c) regularly.

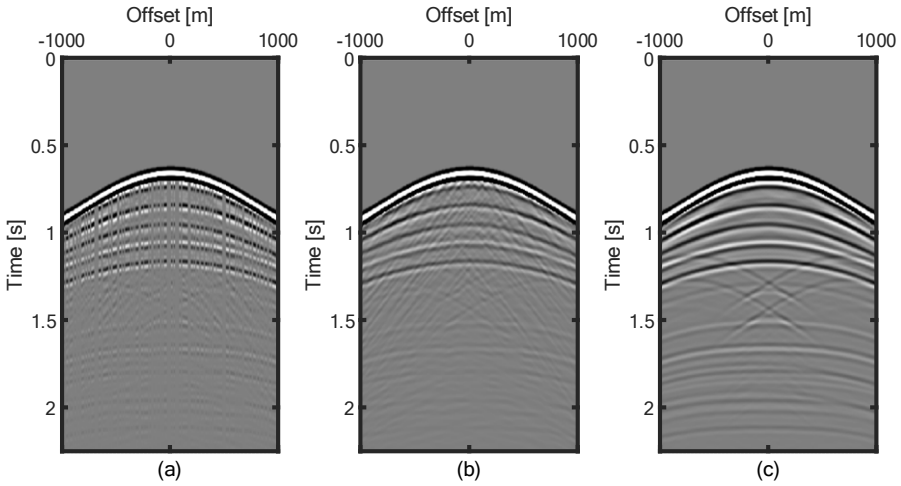

Figure 4. The Green's functions obtained by the standard Marchenko method integrated under the receiver dimension. They are sampled (a) under the source dimension; (b) under the receiver dimension; (c) regularly.

2.3. Sparse reconstruction of focusing functions

Our work focuses on the case of sampling and integrating under the same dimension. Now we introduce sparse inversion theory.

In Compressive Sensing, wavefield reconstruction is achieved through sparse transformation and/or the inversion calculator with sparsity constraints [26]. Focusing functions are composed of mostly continuous events and can be traced in a time-offset plot, so they have many common features with other seismic wavefields. Haindl showed that sparse transformation used for the wavefield reconstruction can also be used for reconstruction of focusing functions [25].

Since our goal is to solve a redatuming problem with irregularly sampled input data (*i.e.*, reflection response), now we turn to deal with sparse reconstruction of focusing functions using reflection data with random gaps. We record the vector forms of the complete reflection response and the focusing function as $\boldsymbol{r}$ and $\boldsymbol{f}$ respectively, then the vector forms of the missing reflection response are:

$$\hat{\boldsymbol{r}} = \Phi \boldsymbol{r}, \tag{5}$$

where $\boldsymbol{r} \in \boldsymbol{R}^N$, $\hat{\boldsymbol{r}} \in \boldsymbol{R}^M$, $N > M$. $\Phi \in \boldsymbol{R}^{M \times N}$ is the sampling matrix. $\hat{\boldsymbol{r}}$ will also cause the gaps in the follow-up focusing function, which is expressed as $\hat{\boldsymbol{f}}$. It follows

Preprints (www.preprints.org) | NOT PEER-REVIEWED | Posted: 5 December 2022 doi:10.20944/preprints202212.0055.v1

$$\hat{\boldsymbol{f}} = \Phi \boldsymbol{f}. \tag{6}$$

Assuming that $\boldsymbol{f}$ can be represented sparsely in the transform domain, the transform domain is called sparse domain. Then we have

$$\boldsymbol{a} = \Psi \boldsymbol{f}, \tag{7}$$

where Ψ is the sparse basis, and $\boldsymbol{a}$ is the sparse coefficient of $\boldsymbol{f}$ in the sparse domain. Substitute Equation 7 into Equation 6 and we get

$$\hat{\boldsymbol{f}} = \Theta \boldsymbol{a}, \tag{8}$$

where $\Theta = \Phi \Psi^{-1}$. Ψ^{-1} is the inverse of Ψ. Θ is usually called recovery matrix. Since $N > M$, Equation 8 is underdetermined and has infinite solutions, so it is impossible to reconstruct the complete focusing function. However, if the recovery matrix Θ satisfies the Restricted Isometry Property (RIP), we can obtain the unique solution. When the sampling matrix Φ is incoherent with the sparse basis Ψ, this property can be satisfied. Therefore, to reconstruct the complete focusing function, the direct way is to solve the L0-norm through continuous optimization:

$$\tilde{\boldsymbol{a}} = \arg\min_{\boldsymbol{a}} \left\| \boldsymbol{a} \right\|_0 \qquad s.t. \left\| \Theta \boldsymbol{a} - \hat{\boldsymbol{f}} \right\|_2 \le \sigma, \tag{9}$$

where $\tilde{\boldsymbol{a}}$ is the optimal sparse coefficient, σ is the reconstruction error, and the constraint condition $\left\| \Theta \boldsymbol{a} - \hat{\boldsymbol{f}} \right\|_2 \le \sigma$ ensures that the solution converges to the true value. Equation 9 is an underdetermined ill-posed problem. It is difficult to obtain an accurate solution. However, L0-norm and L1-norm can get the same approximate solution under a certain condition [27], so Equation 9 is transformed into a convex optimization problem:

$$\tilde{\boldsymbol{a}} = \arg\min_{\boldsymbol{a}} \left\| \boldsymbol{a} \right\|_1 \qquad s.t. \left\| \Theta \boldsymbol{a} - \hat{\boldsymbol{f}} \right\|_2 \le \sigma, \tag{10}$$

Then the reconstructed focusing function can be obtained by

$$\tilde{\boldsymbol{f}} = \Psi^{-1} \tilde{\boldsymbol{a}}. \tag{11}$$

2.4. Sparse Inversion In Iterative Marchenko Scheme

We propose the workflow (Figure 5) referring to the work of IJsseldijk [24]. Our method reconstructs focusing functions in each iteration. The first step is to estimate the initial downgoing focusing function $f_{1,0}^{+}$ to start the iteration. To facilitate calculation, it is usually approximated by the time reversal of the direct arrival of the Green's function G_d [28]:

$$f_{1,0}^{+}(\mathbf{x}_R, \mathbf{x}_A, t) \approx G_d(\mathbf{x}_R, \mathbf{x}_A, -t), \tag{12}$$

This approximation mainly means that the transmission losses at the interfaces are ignored.

Next, the focusing functions are calculated according to Equation 4. The downgoing focusing function is retrieved from the initial condition of the first iteration, or from the upgoing focusing function that is cross-correlated with the reflection response in the last iteration; the upgoing focusing function is the convolution of the downgoing focusing function and the reflection response. We use a time windowing operator θ to separate focusing functions from Green's functions. θ removes all energy whose arrival time is greater than or equal to the direct arrival time.

In steps 3, 4, 6 and 7, we reconstruct $\hat{f}_1^{\pm}$ and $\hat{G}^{\pm}$ in Equation 4 by introducing sparse inversion. According to Equations 10 and 11, the reconstruction problem can be expressed as follows:

$$\begin{aligned} &\tilde{G}^{\pm}(\mathbf{x}_A, \mathbf{x}_S, t) \mp \tilde{f}_1^{\pm}(\mathbf{x}_S, \mathbf{x}_A, \mp t) = \Psi^{-1} \arg\min_{\mathbf{a}^{\mp}} \left\| \mathbf{a}^{\mp} \right\|_1 \\ &s.t. \left\| \Theta \mathbf{a}^{\mp} \pm \sum_i R(\mathbf{x}_R^{(i)}, \mathbf{x}_S, t) * f_1^{\mp}(\mathbf{x}_R^{(i)}, \mathbf{x}_A, \mp t) * S(t) \right\|_2 \le \sigma, \end{aligned} \tag{13}$$

where $\tilde{f}_1^{\pm}$ and $\tilde{G}^{\pm}$ are the recovered focusing functions and Green's functions. This equation is the iterative Marchenko scheme with sparse inversion proposed in this paper.

Preprints (www.preprints.org) | NOT PEER-REVIEWED | Posted: 5 December 2022 doi:10.20944/preprints202212.0055.v1

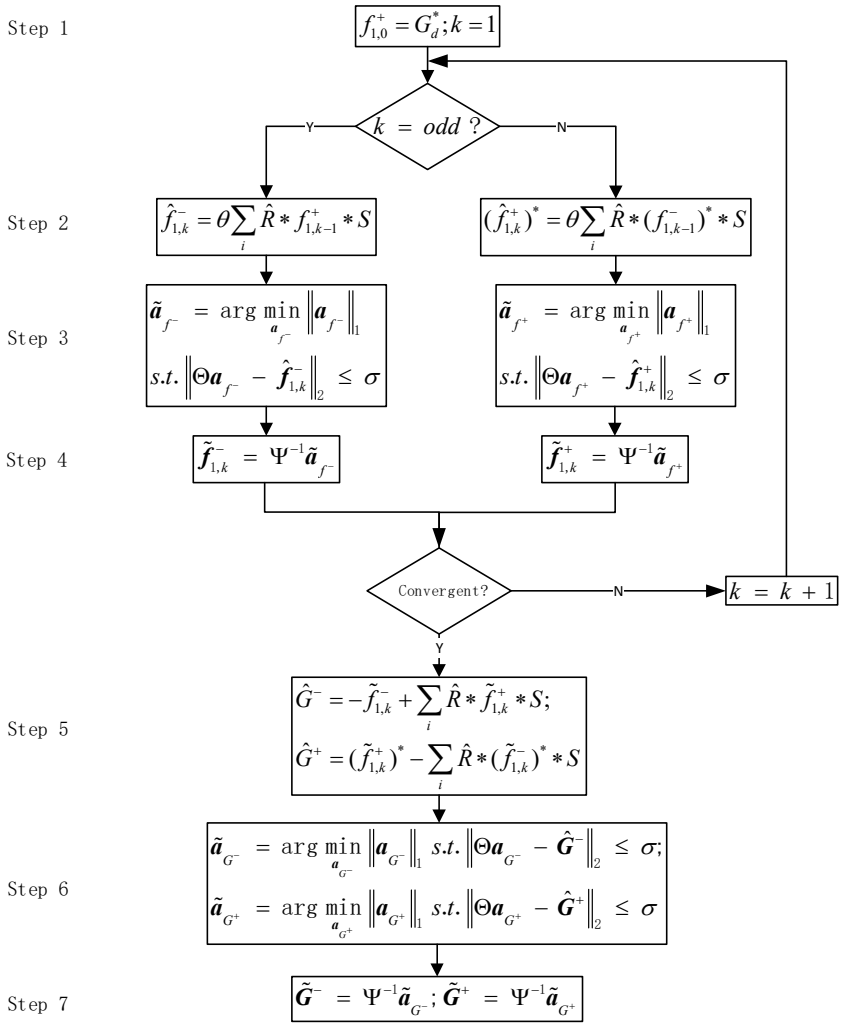

Figure 5. Workflow of the proposed Marchenko method. The focusing functions and Green's functions are recovered by Step 3, 4, 6 and 7. S is the source signal, k is the number of iterations, the superscript asterisk is the time reversal, the internal asterisk is the convolution or correlation, and θ is the time window operator.

3. Numeral examples

The performance of our method is tested on the synthetic data. This test uses the same two-dimensional model as above (Figure 1). For irregularly sampling, 40% of the sources are randomly removed, and the sampling mask is shown in Figure 2a. The direct arrival of the Green's function between the source depth and the surface is estimated in the smooth model. As previously mentioned, the time reversal of direct arrival is used for the initial estimation of the downgoing focusing function. The reflection response and the initial estimate are the inputs required for the iterative Marchenko scheme. For the third and sixth steps of our method, we need to know the locations of the missing sources.

We use the SPGL1 solver [29] to invert Equation 13 in Fourier transform, wavelet transform and curvelet transform. Figure 6 compares the convergence in these domains. It can be seen that the results of sparse reconstruction using wavelet transform (red line) are the worst, while Fourier transform (blue line) converges gradually after 50 iterations. From the overall results and convergence, the best effect is curvelet transform (yellow line), which starts to converge after 200 iterations. This shows that the focusing function is particularly sparse in the curvelet domain, because the SPGL1 solver gradually loosens the sparsity constraint to facilitate smaller mismatches. Figure 7 shows the reconstructed focusing functions obtained by these three transforms. It can be clearly seen that the focusing function reconstructed with the curvelet transform (Figure 7d) is the most similar to the reference figure (Figure 7e).

Preprints (www.preprints.org) | NOT PEER-REVIEWED | Posted: 5 December 2022 doi:10.20944/preprints202212.0055.v1

After determining that the curvelet domain is the best transform domain in our method, we use the FISTA sparse solver [30] to invert Equation 13 as well. Figure 8 shows the convergence of the SPGL1 solver and the FISTA solver with curvelet transform. It can be seen that the FISTA solver (blue line) becomes flat after nearly 50 iterations, while the SPGL1 solver (red line) needs more than 300 iterations to achieve better results than the FISTA solver. Hence, we choose the results of 50 iterations with FISTA solver to continue the calculation. We compare the final Green's functions obtained by the standard Marchenko method and our method in Figure 9. It can be seen that the gaps caused in the standard Marchenko method (Figure 9a) are effectively filled in our method (Figure 9b). To facilitate observation, in Figure 10, we enlarge the single traces of the three Green's functions in Figure 9, which are represented by blue lines, red lines and yellow lines, respectively. We can see that the reconstructed Green's functions (red lines) and the reference Green's functions (yellow lines) are well matched at the near offset x = 10 m (Figure 10a) and the far offset x = -960 m (Figure 10b).

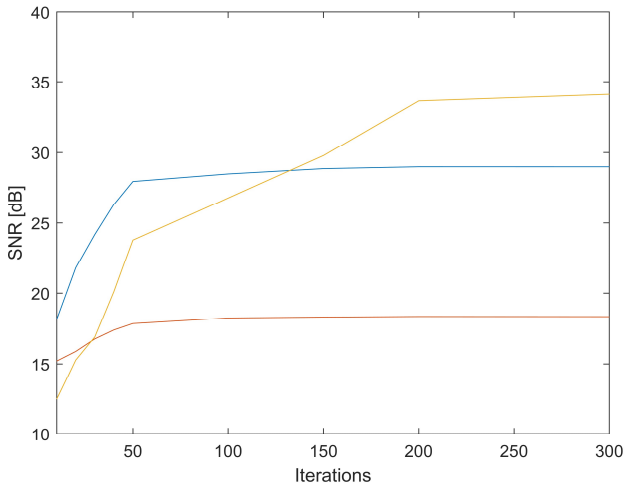

Figure 6. Comparison of convergence of SPGL1 algorithm in sparse reconstruction of focusing functions, in which the red line is wavelet transform, the blue line is Fourier transform, and the yellow line is curvelet transform.

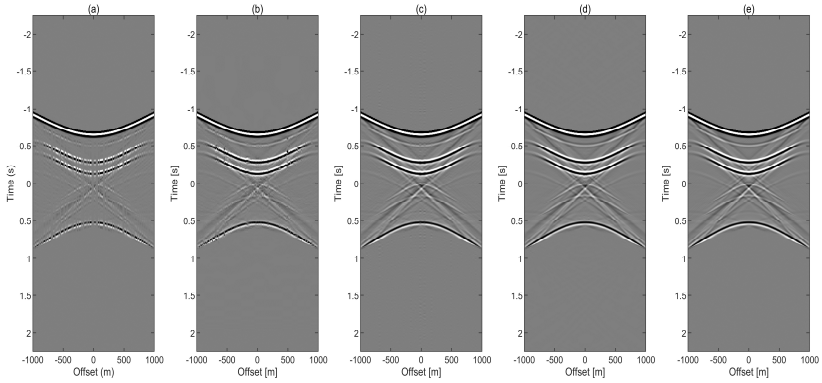

Figure 7. Comparison of reconstructed focusing functions. (a) The focusing function without reconstruction calculated by irregular sampling over the source dimension and integrating over the receiver dimension; (b) The reconstructed focusing function for sparse reconstruction in wavelet domain (50 iterations); (c) The reconstructed focusing function for sparse reconstruction in Fourier domain (50 iterations); (d) The reconstructed focusing function for sparse reconstruction in curvelet domain (200 iterations); (e) The focusing function for reference.

Preprints (www.preprints.org) | NOT PEER-REVIEWED | Posted: 5 December 2022 doi:10.20944/preprints202212.0055.v1

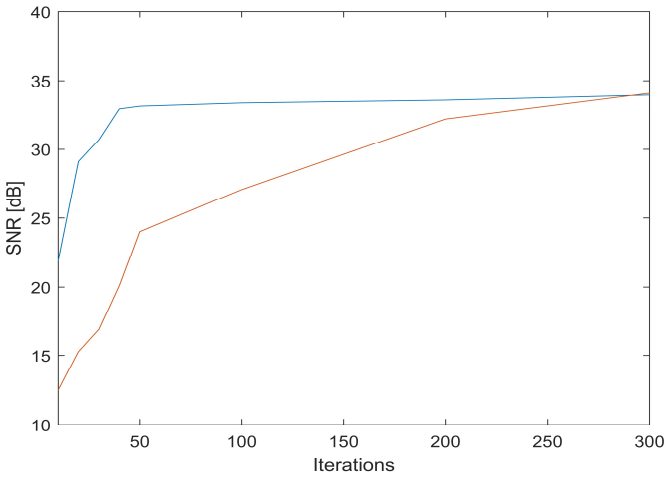

Figure 8. Comparison of convergence of the SPGL1 solver (red line) and the FISTA solver (blue line) in curvelet transform for focusing function reconstruction.

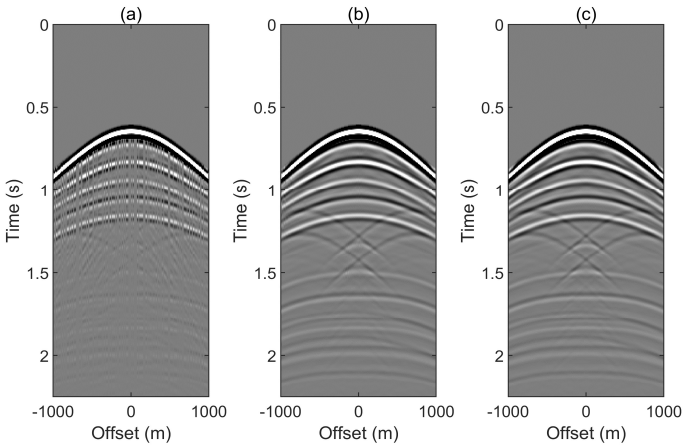

Figure 9. Comparison of the Green's functions. (a) is obtained by the standard Marchenko method with irregular sampling; (b) is obtained by our improving Marchenko method with sparse reconstruction; (c) is the reference Green's function.

Preprints (www.preprints.org) | NOT PEER-REVIEWED | Posted: 5 December 2022 doi:10.20944/preprints202212.0055.v1

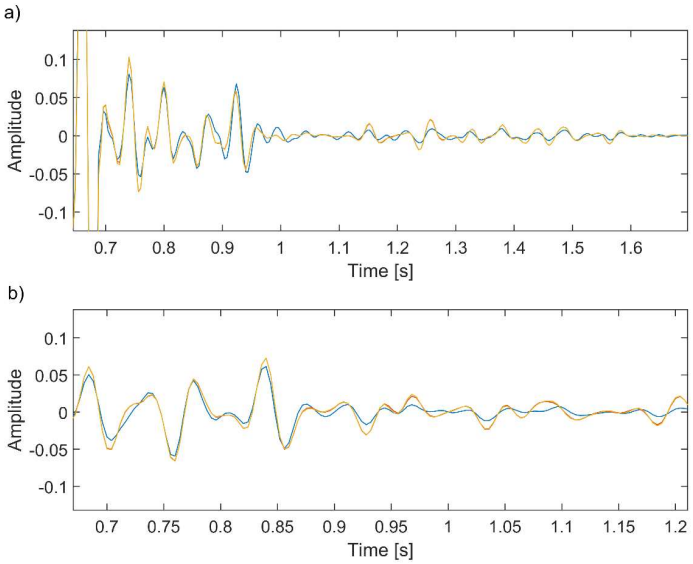

Figure 10. To compare the amplified traces of the Green's functions of figure 9a, 9b and 9c which are blue, red and yellow, respectively. They are at (a) near offset x = 10 m and (b) far offset x = -960 m.

4. Discussion

When the Marchenko method is used for seismic data sets with gaps in the acquisition geometry, sparse reconstruction for wavefields can also be used as a preprocessing process, resulting in a higher noise level of Green's functions [25]. However, preprocessing requires sparse reconstruction of all shots, which has a higher computational cost.

Some papers have already combined the Marchenko method with sparse inversion [25,31,32]. But they need to directly invert the Marchenko equations. When the amount of data is large, the inverse of the matrix in inversion is difficult to solve. Therefore, we choose to integrate sparse inversion into the iterative Marchenko scheme because of its simpler calculation. IJsseldijk's method [24] also uses the iterative scheme. But what it deals with is the situation where sampling and integrating under the same dimensions. Perhaps our method can be combined with IJsseldijk's iterative method to deal with two cases of sampling and integration in different and the same dimensions.

5. Conclusions

One limitation of the standard Marchenko method is the need for well-sampled and collocated sources and receivers. This paper broadens this requirement and proves that the obtained focusing functions and Green's functions can be improved by sparse inversion when there are randomly distributed gaps in the input of the Marchenko method. For this method, we need to know the locations of the missing sources. We extend four steps (Steps 3, 4, 6 and 7) in each iteration of the standard Marchenko method. Compared with directly inverting the sparse constrained Marchenko equation, the complexity is reduced.

Author Contributions: Conceptualization, J.Z. and L.H.; methodology, J.Z.; software, J.Z; validation, J.Z.; writing—original draft preparation, J.Z.; writing—review and editing, J.Z. and L.H.; supervision, L.H.; project administration, L.H.; funding acquisition, L.H. All authors have read and agreed to the published version of the manuscript.

Funding: This research was funded by the National Natural Science Foundation of China, grant number 42074154 and 42130805.

Data Availability Statement: Not applicable.

Conflicts of Interest: The authors declare no conflict of interest

References

1. E. Slob, K. Wapenaar, F. Broggini, and R. Snieder, "Seismic reflector imaging using internal multiples with Marchenko-type equations," GEOPHYSICS, vol. 79, no. 2, pp. S63–S76, 2014, doi: 10.1190/geo2013-0095.

2. K. Wapenaar, J. Thorbecke, J. van der Neut, F. Broggini, E. Slob, and R. Snieder, "Marchenko imaging," GEOPHYSICS, vol. 79, no. 3, pp. WA39-WA57, 2014, doi: 10.1190/geo2013-0302.1.
3. K. Wapenaar et al., "Marchenko redatuming, imaging, and multiple elimination and their mutual relations," GEOPHYSICS, vol. 86, no. 5, pp. WC117-WC140, 2021, doi: 10.1190/geo2020-0854.1.
4. Marchenko V A. On reconstruction of the potential energy from phases of the scattered waves[C]//Dokl. Akad. Nauk SSSR. 1955, 104(5): 695-698.
5. Burridge R. The Gelfand-Levitan, the Marchenko, and the Gopinath-Sondhi integral equations of inverse scattering theory, regarded in the context of inverse impulse-response problems[J]. Wave motion, 1980, 2(4): 305-323.
6. Chadan K, Sabatier P C. Inverse problems in quantum scattering theory[M]. Springer Science & Business Media, 2012.
7. F. Broggini and R. Snieder, "Connection of scattering principles: a visual and mathematical tour," *European Journal of Physics*, vol. 33, no. 3, pp. 593–613, 2012, doi: 10.1088/0143-0807/33/3/593.
8. Bakulin A, Calvert R. The virtual source method: Theory and case study[J]. Geophysics, 2006, 71(4): SI139-SI150.
9. Curtis A, Gerstoft P, Sato H, et al. Seismic interferometry—Turning noise into signal[J]. The Leading Edge, 2006, 25(9): 1082-1092.
10. Snieder R, Wapenaar K, Larner K. Spurious multiples in seismic interferometry of primaries[J]. Geophysics, 2006, 71(4): SI111-SI124.05620.
11. K. Wapenaar, F. Broggini, E. Slob, and R. Snieder, "Three-Dimensional Single-Sided Marchenko Inverse Scattering, Data-Driven Focusing, Green's Function Retrieval, and their Mutual Relations," Physical Review Letters, vol. 110, no. 8, 2013, doi: 10.1103/physrevlett.110.084301.
12. K. Wapenaar and E. Slob, "On the Marchenko equation for multicomponent single-sided reflection data," Geophysical Journal International, vol. 199, no. 3, pp. 1367–1371, 2014, doi: 10.1093/gji/ggu313.
13. R. U. C, "Elastodynamic Marchenko inverse scattering: A multiple-elimination strategy for imaging of elastodynamic seismic reflection data," 2020.
14. S. Singh, R. Snieder, J. Behura, J. van der Neut, K. Wapenaar, and E. Slob, "Marchenko imaging: Imaging with primaries, internal multiples, and free-surface multiples," GEOPHYSICS, vol. 80, no. 5, pp. S165–S174, 2015, doi: 10.1190/geo2014-0494.1.
15. E. Slob, "Green's Function Retrieval and Marchenko Imaging in a Dissipative Acoustic Medium," Physical Review Letters, vol. 116, no. 16, 2016, doi: 10.1103/physrevlett.116.164301.
16. J. Behura, K. Wapenaar, and R. Snieder, "Autofocus Imaging: Image reconstruction based on inverse scattering theory," GEOPHYSICS, vol. 79, no. 3, pp. A19–A26, 2014, doi: 10.1190/geo2013-0398.1.
17. J. van der Neut, K. Wapenaar, J. Thorbecke, E. Slob, and I. Vasconcelos, "An illustration of adaptive Marchenko imaging," The Leading Edge, vol. 34, no. 7, pp. 818–822, 2015, doi: 10.1190/tle34070818.1.
18. G. A. Meles, K. Wapenaar, and A. Curtis, "Reconstructing the primary reflections in seismic data by Marchenko redatuming and convolutional interferometry," GEOPHYSICS, vol. 81, no. 2, pp. Q15–Q26, 2016, doi: 10.1190/geo2015-0377.1.
19. L. Zhang and E. Slob, "Free-surface and internal multiple elimination in one step without adaptive subtraction," GEOPHYSICS, vol. 84, no. 1, pp. A7–A11, 2019, doi: 10.1190/geo2018-0548.1.
20. L. Zhang, J. Thorbecke, K. Wapenaar, and E. Slob, "Transmission compensated primary reflection retrieval in the data domain and consequences for imaging," GEOPHYSICS, vol. 84, no. 4, pp. Q27–Q36, 2019, doi: 10.1190/geo2018-0340.1.
21. M. Ravasi, "Rayleigh-Marchenko redatuming for target-oriented, true-amplitude imaging," GEOPHYSICS, vol. 82, no. 6, pp. S439–S452, 2017, doi: 10.1190/geo2017-0262.1.
22. H. Peng and I. Vasconcelos, "A study of acquisition-related sub-sampling and aperture effects on Marchenko focusing and redatuming," 2019. doi: 10.1190/segam2019-3214965.1.
23. K. Wapenaar and J. van IJsseldijk, "Discrete representations for Marchenko imaging of imperfectly sampled data," GEOPHYSICS, vol. 85, no. 2, pp. A1–A5, 2020, doi: 10.1190/geo2019-0407.1.
24. J. van IJsseldijk and K. Wapenaar, "Adaptation of the iterative Marchenko scheme for imperfectly sampled data," Geophysical Journal International, vol. 224, no. 1, pp. 326–336, 2020, doi: https://doi.org/10.1093/gji/ggaa463.
25. C. Haindl, M. Ravasi, and F. Broggini, "Handling gaps in acquisition geometries — Improving Marchenko-based imaging using sparsity-promoting inversion and joint inversion of time-lapse data," GEOPHYSICS, vol. 86, no. 2, pp. S143–S154, 2021, doi: 10.1190/geo2020-0036.1.
26. Hennenfent G, Herrmann F J. Simply denoise: Wavefield reconstruction via jittered undersampling[J]. Geophysics, 2008, 73(3): V19-V28.
27. Donoho D L. Compressed sensing[J]. IEEE Transactions on information theory, 2006, 52(4): 1289-1306.
28. J. Thorbecke, E. Slob, J. Brackenhoff, J. van der Neut, and K. Wapenaar, "Implementation of the Marchenko method," GEOPHYSICS, vol. 82, no. 6, pp. WB29-WB45, 2017, doi: 10.1190/geo2017-0108.1.
29. Van den Berg E, Friedlander M P. SPGL1: A solver for large-scale sparse reconstruction[J]. 2007.
30. Beck A, Teboulle M. A fast iterative shrinkage-thresholding algorithm for linear inverse problems[J]. SIAM journal on imaging sciences, 2009, 2(1): 183-202.
31. H. CM, B. Filippo, R. M, and van M. D-J, "Using sparsity to improve the accuracy of Marchenko imaging given imperfect acquisition geometries," in 80th EAGE Conference and Exhibition 2018, 2018, vol. 2018, no. 1, pp. 1--5.
32. M. Zhang, "Compressive Sensing Acquisition with Application to Marchenko Imaging," Pure and Applied Geophysics, vol. 179, no. 6–7, pp. 2383–2404, 2022, doi: 10.1007/s00024-022-03029-5.